www.nature.com/cdd

ARTICLE

E3 ligase RNF99 negatively regulates TLR-mediated inflammatory immune response via K48-linked ubiquitination of TAB2

Jie Zhang[1,3], Lei Cao[1,3], Amy Gao[1], Ruiqing Ren[1], Liwen Yu[1], Qian Li[1], Yapeng Liu[1], Wenqian Qi[1], Yonghao Hou[1], Wenhai Sui[1], Guohai Su[2], Yun Zhang[1,2], Cheng Zhang[1,2]✉ and Meng Zhang[1,2]✉

Innate immunity is the first line to defend against pathogenic microorganisms, and Toll-like receptor (TLR)-mediated inflammatory responses are an essential component of innate immunity. However, the regulatory mechanisms of TLRs in innate immunity remain unperfected. We found that the expression of E3 ligase Ring finger protein 99 (RNF99) decreased significantly in peripheral blood monocytes from patients infected with Gram negative bacteria (G^-) and macrophages stimulated by TLRs ligands, indicating the role of RNF99. We also demonstrated for the first time, the protective role of RNF99 against LPS-induced septic shock and dextran sodium sulfate (DSS)-induced colitis using RNF99 knockout mice ($RNF99^{-/-}$) and bone marrow-transplanted mice. In vitro experiments revealed that RNF99 deficiency significantly promoted TLR-mediated inflammatory cytokine expression and activated the NF-κB and MAPK pathways in macrophages. Mechanistically, in both macrophages and HEK293 cell line with TLR4 stably transfection, RNF99 interacted with and degraded TAK1-binding protein (TAB) 2, a regulatory protein of the kinase TAK1, via the lysine (K)48-linked ubiquitin-proteasomal pathway on lysine 611 of TAB2, which further regulated the TLR-mediated inflammatory response. Overall, these findings indicated the physiological significance of RNF99 in macrophages in regulating TLR-mediated inflammatory reactions. It provided new insight into TLRs signal transduction, and offered a novel approach for preventing bacterial infections, endotoxin shock, and other inflammatory ills.

Cell Death & Differentiation (2023) 30:966–978; https://doi.org/10.1038/s41418-023-01115-2

INTRODUCTION

Activation of the innate immune system requires pattern recognition receptors (PRPs) to recognize pathogen-associated molecular patterns (PAMPs), and macrophages are the main effector cells [1]. Toll-like receptors (TLRs), the earliest discovered and most studied pattern recognition receptors, are bacterial sensors that act as interfaces between the external environment and cell responses [2]. Once TLRs recognize conserved microbe-associated motifs, macrophages secrete proinflammatory factors such as TNF-α, IL-1β, and IL-6, which conversely contribute to further activation of inflammatory signaling [3, 4]. Abnormal TLRs signal transduction can lead to abnormal inflammatory responses and many related immune diseases, including sepsis and inflammatory bowel disease (IBD) [5–7]. It is a pathological syndrome characterized by persistent excessive inflammation and immunosuppression and associated with high morbidity and mortality. TLR agonists have shown great potential as antimicrobial agents and vaccine adjuvants, while TLR antagonists are being developed as reagents and drugs to inhibit immune response. And previous studies have shown that TLR4 can be used as a therapeutic target in sepsis [7–9]. Although the understanding of the key pathogenesis of TLR-mediated human disease has greatly increased, there is still a lack of a fully effective clinical treatment. Therefore, it is important to explore the mechanism of TLRs signaling and avoid abnormal activation of TLR signals.

When TLRs are stimulated by ligands such as lipopolysaccharide (LPS) (TLR4 ligand), R848 (Resiquimod) (TLR7/8 ligand), and lipoteichoic acid (LTA) (TLR2 ligand), they initiate a signaling cascade by recruiting MyD88 or TRIF. MyD88 triggers the formation and activation of TAK1-TABs complexes and leads to the phosphorylation of the nuclear factors NF-κB and MAPKs [4, 10, 11]. Eventually, immune and inflammatory responses, fever, endotoxemia, and shock are initiated. Studies have shown that TAK1 plays a critical role in tumor necrosis factor receptor (TNFR), interleukin-1 receptor I (IL-1RI), and TLR-mediated NF-κB and MAPKs activations [12]. TAK1 activation requires TAK1-binding proteins (TAB1, TAB2, and TAB3), and the TAK1-TABs complex plays an essential role in innate immune and inflammatory responses [13–15]. Although the TAK1-TAB complex has been extensively studied, the role of individual proteins

[1]The Key Laboratory of Cardiovascular Remodeling and Function Research, Chinese Ministry of Education, Chinese National Health Commission and Chinese Academy of Medical Sciences, The State and Shandong Province Joint Key Laboratory of Translational Cardiovascular Medicine, Department of Cardiology, Qilu Hospital, Cheeloo College of Medicine, Shandong University, Jinan, Shandong, China. [2]Cardiovascular Disease Research Center, Jinan Central Hospital, Shandong First Medical University, Jinan, Shandong, China. [3]These authors contributed equally: Jie Zhang, Lei Cao. ✉email: zhangc@sdu.edu.cn; zhangmeng@sdu.edu.cn

Received: 18 August 2022 Revised: 23 December 2022 Accepted: 9 January 2023
Published online: 21 January 2023

and their molecular mechanisms of activation in different cell types remain to be elucidated.

Intracellular signaling, through covalent attachment of different ubiquitin-linked protein substrates, underlies many cellular processes [16, 17]. In recent years, increasing evidence has shown that lots of E3 ligases are involved in the regulation of innate immunity and inflammation by modifying TLRs signaling pathway-related proteins. For example, the E3 ligase Nrdp1 can modify MyD88 and TBK1 through ubiquitination, thereby negatively regulating the expression of TLR-mediated pro-inflammatory cytokines [18, 19]. The E3 ligase TRIM38 promotes K48-linked ubiquitination of TRIF and negatively regulates TLR3-mediated IFN-β expression [20]. TRIM38 can also promote K48-linked ubiquitination, degradation of NAP1, and inhibition of IRF3 activation, thus negatively regulating the TLR/RLR-mediated signaling pathways [21]. Ring finger protein 99 (RNF99), a new member of the E3 ligase TRIM family, has rarely been studied. Research have shown that RNF99 functions as a tumor suppressor in the brain via its E3 ligase activity by stabilizing p53 through K63-linked ubiquitination [22]. Meanwhile, studies have shown that RNF99 could negatively regulate NF-κB-mediated transcriptional activity and proliferation of HeLa or NIH3T3 cells, but lack detailed mechanisms and targets for ubiquitination modification [23]. To date, the molecular mechanisms and functions of RNF99 in relation to different diseases need to be further explored.

Considerable evidence suggests the importance of post-translational modifications (PTMs) of TAK1 and TAB in regulating TAK1 activation. So far, aside from phosphorylation, ubiquitination is one of the most widely studied posttranslational modifications [24]. And research have shown that the ubiquitin-proteasome system plays a crucial role in the TAK1-TAB complex assembly and TAK1 activation [25]. But studies on TAB2 degradation have mainly focused on the lysosomal pathway. It has been reported that E3 ligases TRIM38 [26], TRIM30α [27], TRIM22 [28], and RNF4 [29] can target TAB2 and degrade it through the lysosomal pathway. Whether the proteasome pathway is involved in TAB2 degradation has been unclear. Therefore, it is crucial to further explore the specific E3 ubiquitin ligase that promotes TAB2 degradation in the proteasome pathway. It is also important to study the molecular mechanism of its influence on TAB2 ubiquitination and related-TAK1 kinase activity, and clarify its physiological significance in inflammatory diseases such as endotoxemia and colitis.

In our study, it was found that E3 ubiquitin ligase RNF99, as a feedback regulator, could negatively regulates TLRs-mediated inflammatory immune response in macrophages, and then involved in the progression of endotoxemia and colitis in mice. In mechanism, we found that RNF99 could specifically bind to TAB2 and promoted K48-linked ubiquitination at the K611 lysine residue, thereby mediating its degradation through the proteasomal pathway. Through the above studies, we found that E3 ligase RNF99 affects the formation of protein kinase TAK1-TAB1-TAB2 complex and inflammation by regulating TAB2 degradation via ubiquitin-proteasome pathway.

MATERIALS AND METHODS

A detailed method and original western blots with markers are available in the Online Supplemental Materials.

RESULTS

TLRs stimulation and Gram-negative bacillus (G^-) infection decreased expression of RNF99 in macrophages

RNF99 expression and inflammatory response changes were investigated employing various TLR ligand treatments in PMs and BMDMs extracted from wild-type (WT) mice. Both mRNA (Fig. 1A) and protein (Fig. 1B, C) levels of RNF99 were significantly downregulated upon stimulation of the TLR4 ligand (LPS) in PMs and BMDMs. Similar results were obtained in response to different stimulations of TLR7/8 (R848) and TLR2 (LTA) ligands, respectively. This further suggested that RNF99 may be a feedback regulator of TLR-mediated innate immunity.

LPS, a TLR4 ligand, is a key component of the G^- bacterial cell wall [9]. We collected peripheral blood from patients with G^- infection and healthy individuals, and confirmed it through blood culture. $CD14^+$ monocytes were sorted using flow cytometry and detected employing quantitative real-time PCR (RT-PCR). Compared to the healthy participants, mRNA levels of TNF-α, IL-6, and IL-1β in G^- infected patients were significantly higher (Fig. 1D). However, RNF99 levels were decreased (Fig. 1E), suggesting that its expression in monocytes may be closely related to bacterial infections.

RNF99 knockout effect on TLRs-mediated endotoxemia and acute colitis

To determine the role of RNF99 in TLR-mediated innate inflammatory responses, we constructed RNF99 knockout mice ($RNF99^{-/-}$) using CRISPR/Case9 technology (Supplementary Fig. 1A, B). The knockout efficiency of PMs was confirmed using western blotting (Supplementary Fig. 1C). LPS-induced endotoxemia and lung injury in vivo model was established to study TLR-related molecular mechanisms and potential therapies for inflammation-related lung injury. We then constructed a mouse endotoxemia model by intraperitoneal injection of LPS. Compared with WT littermate controls ($RNF99^{+/+}$), RNF99 knockout mice significantly aggravated polymorphonuclear cell infiltration and interstitial pneumonitis in the lungs after the LPS challenge (Fig. 2A, B). The production of TNF-α, IL-6, and IL-1β in the sera from $RNF99^{-/-}$ mice was also significantly upregulated after TLR challenge (Fig. 2C). In response to lethal challenge with LPS, $RNF99^{-/-}$ mice experienced earlier onset of death and exhibited higher mortality (Fig. 2D). These data suggested that RNF99 negatively regulates endotoxin-mediated inflammatory diseases in vivo.

Abnormal intestinal flora induces activation of macrophage TLRs signaling and mediates inflammatory response, which is an important event for the development of IBD [5, 30]. DSS-induced colitis is a classic inflammatory model used to investigate the mechanisms of IBD [31, 32]. Hence, we further studied the effect of RNF99 deficiency on the DSS-mediated inflammatory response. The results showed that, compared with $RNF99^{+/+}$ mice, the clinical manifestations of colitis in $RNF99^{-/-}$ mice were significantly aggravated, mainly manifested as weight loss in 6–7 days (Fig. 2E), soft stool in 5–7 days (Fig. 2F), and aggravated hematochezia in 5–7 days (Fig. 2G), at the same time, the colon of mice was shortened (Fig. 2H, I). Histopathological examination by H&E staining of the colon sections revealed aggravated mucosal destruction and increased inflammatory cell infiltration in $RNF99^{-/-}$ mice (Fig. 2J, K). In addition, the expression of proinflammatory factors in the peripheral blood of $RNF99^{-/-}$ mice was significantly upregulated (Fig. 2L). Collectively, RNF99 deficiency significantly aggravated the severity of TLR-mediated endotoxemia and acute colitis.

Regulation of TLRs-mediated inflammatory diseases by RNF99 in macrophages

To further demonstrate that the RNF99 specifically in macrophages plays a key role in TLR-mediated inflammatory diseases, we transplanted bone marrow cells from $RNF99^{+/+}$ or $RNF99^{-/-}$ mice donors into irradiated $RNF99^{+/+}$ mice ($RNF99^{+/+} \rightarrow RNF99^{+/+}$ or $RNF99^{-/-} \rightarrow RNF99^{+/+}$) (Fig. 3A), or transplanted bone marrow cells from $RNF99^{+/+}$ or $RNF99^{-/-}$ mice into irradiated $RNF99^{-/-}$ mice

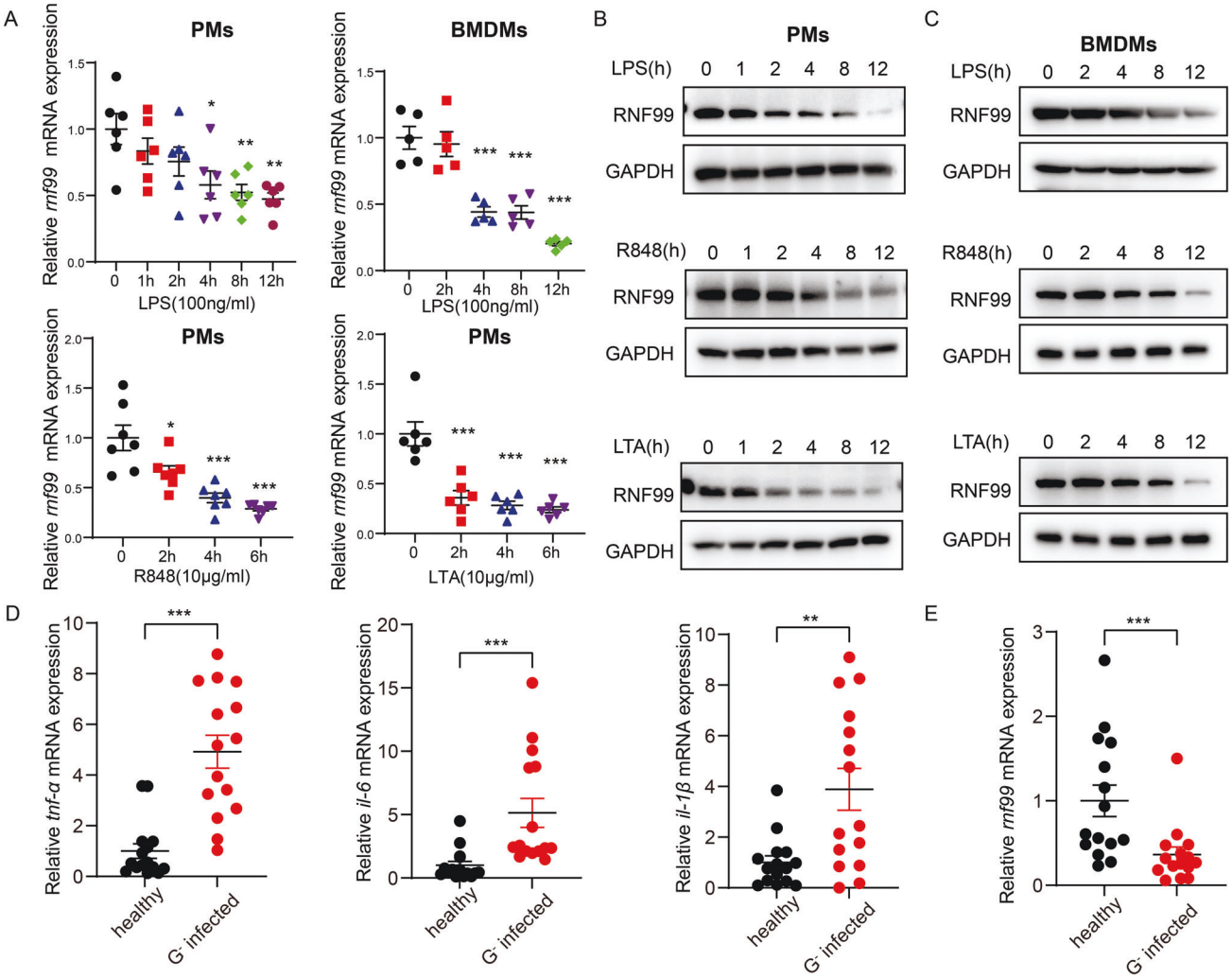

Fig. 1 Gram negative (G⁻) infection and TLRs stimulation decreased expression of RNF99 in macrophages. A Relative *rnf99* mRNA levels in PMs and BMDMs stimulated by LPS ($n = 5$–6), R848 ($n = 7$), or LTA ($n = 6$) for different periods of time. **B, C** Representative western blot images of RNF99 in PMs and BMDMs after LPS, R848, or LTA stimulation for different periods of time. **D** Relative mRNA levels of *tnf-α*, *il-6*, and *il-1β* in peripheral blood monocytes of healthy and G⁻ infected patients ($n = 15$). **E** Relative *rnf99* mRNA levels in the peripheral blood monocytes of healthy and G⁻ infected patients ($n = 15$). Data were presented as the mean ± SEM and Gaussian distributions were evaluated by the Shapiro–Wilk method. One-way ANOVA with Dunnett's post hoc test was used for Fig. 1A (LPS-induced PMs and BMDMs, and R848-induced PMs). The Kruskal–Wallis test with Dunnett's post hoc test was used for Fig. 1A (LTA-induced PMs). The Mann–Whitney test was used for Fig. 1D, E. $^{*}P < 0.05$, $^{**}P < 0.01$, $^{***}P < 0.001$. Adjusted P values are provided for multiple group comparisons.

(RNF99$^{+/+}$ → RNF99$^{-/-}$ or RNF99$^{-/-}$ → RNF99$^{-/-}$) (Fig. 3H). The chimeric mice were then challenged with LPS to induce endotoxemia or DSS to induce acute colitis. Compared to RNF99$^{+/+}$ → RNF99$^{+/+}$ mice, RNF99$^{-/-}$ → RNF99$^{+/+}$ counterparts showed severe lung injury in H&E-stained lung sections (Fig. 3B, Supplementary Fig. 2A) and increased proinflammatory factor production after the LPS challenge (Fig. 3C). Consistently, RNF99$^{-/-}$ → RNF99$^{-/-}$ mice also showed aggravated lung inflammation (Fig. 3I) and increased proinflammatory factor production (Fig. 3J) compared to RNF99$^{+/+}$ → RNF99$^{-/-}$ mice after LPS challenge. After DSS-induced colitis was established, clinical and pathological changes in mice showed that, compared with RNF99$^{+/+}$ → RNF99$^{+/+}$ mice, RNF99$^{-/-}$ → RNF99$^{+/+}$ mice displayed aggravated weight loss, soft stool, hematochezia (Fig. 3D), shortened colon (Fig. 3E), mucosal destruction, increased inflammatory cell infiltration (Fig. 3F, Supplementary Fig. 2B) and proinflammatory factor production (Fig. 3G). A similar phenomenon was observed in RNF99$^{-/-}$ → RNF99$^{-/-}$ mice compared to RNF99$^{+/+}$ → RNF99$^{-/-}$ mice (Fig. 3K–N, Supplementary Fig. 2C, D). These results suggested that mice with RNF99$^{-/-}$ bone marrow cells were more sensitive to LPS-induced endotoxin and DSS-induced colitis. Overall, the above results demonstrated the crucial role of macrophage-derived RNF99 in the protection against TLR-triggered inflammatory diseases.

RNF99 deficiency positively regulates TLR-mediated inflammatory cytokine production in macrophages

As an important E3 ubiquitin ligase, the role of macrophage RNF99 in the TLR-mediated immune response remains unclear. To clarify this, PMs and BMDMs were extracted from RNF99$^{+/+}$ and RNF99$^{-/-}$ mice, respectively, and the production of the corresponding inflammatory factors was observed after treatment with different TLR ligands, such as LPS, R848, and LTA. The results showed that, compared to RNF99$^{+/+}$ mice PMs, RNF99$^{-/-}$ mice significantly upregulated mRNA levels of TNF-α, IL-6, and IL-1β after stimulation by LPS (Fig. 4A, B), R848 (Fig. 4C, D), and LTA (Fig. 4E, F). Similar results were obtained from RNF99$^{-/-}$ mouse BMDMs following LPS stimulation (Supplementary Fig. 3A, B).

The production of TLR-mediated inflammatory factors such as TNF-α, IL-6, and IL-1β mainly depends on the activation and transduction of NF-κB and MAPKs. PMs and BMDMs from RNF99$^{+/+}$ and RNF99$^{-/-}$ mice were treated with LPS, R848, or LTA. Western

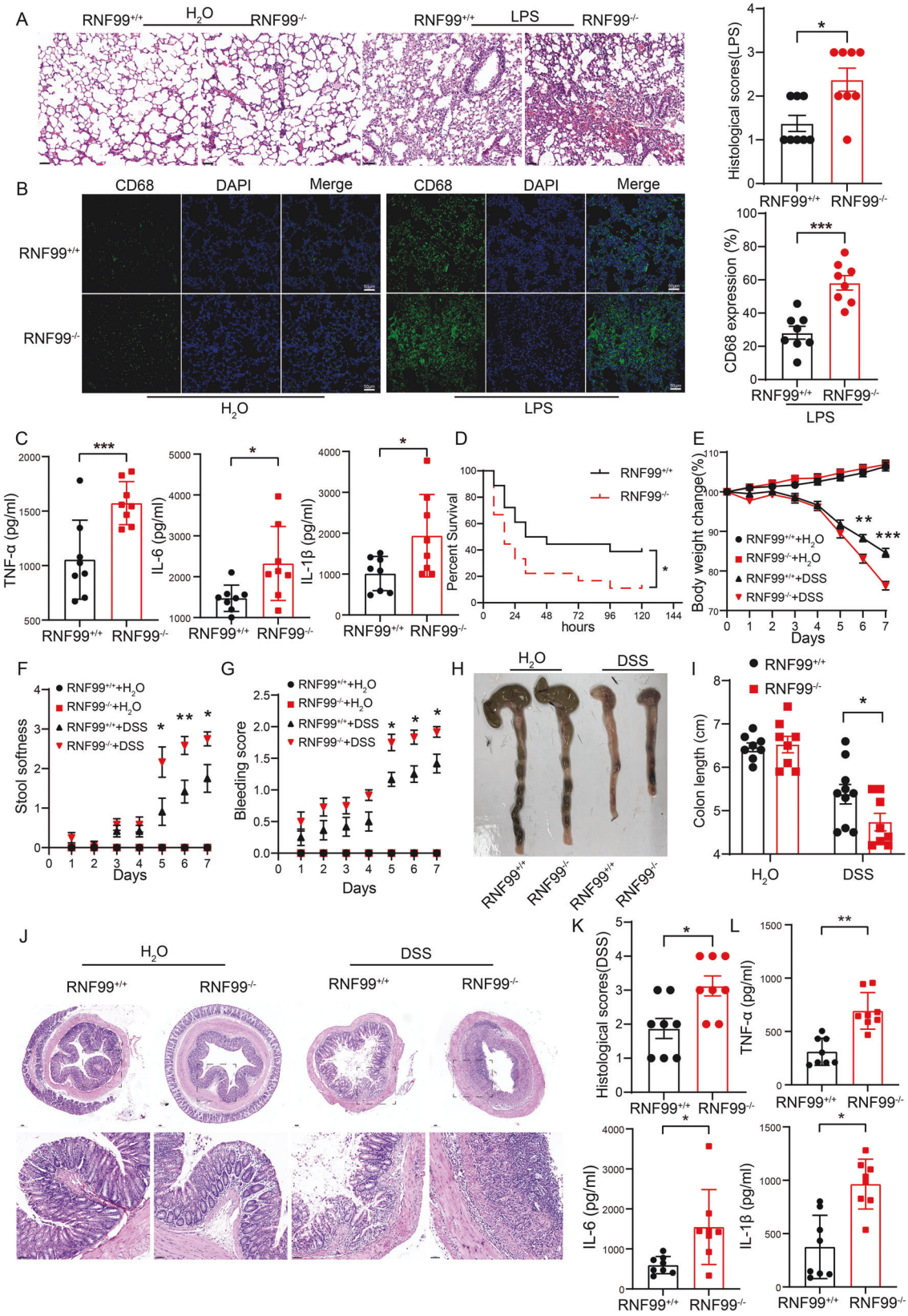

blotting showed that compared with RNF99$^{+/+}$ mouse macrophage, the phosphorylation of IκB-α, P65, an activation hallmark of NF-κB, and phosphorylation of ERK, JNK, P38, hallmarks of MAPK activation, were all significantly increased in the PMs (Fig. 4G, H) and BMDMs (Fig. 4I, J) of RNF99 knockout mice after TLR ligand treatment. The results confirmed that RNF99 deficiency in macrophages enhanced the TLR-induced activation of the NF-κB and MAPK signaling pathways.

Fig. 2 RNF99 knockout significantly aggravated TLR-mediated endotoxemia and acute colitis. Sex- and age-matched RNF99$^{+/+}$ and RNF99$^{-/-}$ mice were intraperitoneally injected with lipopolysaccharide (LPS) or PBS. **A** H&E staining and histopathological analysis of lung sections in RNF99$^{+/+}$ and RNF99$^{-/-}$ mice after LPS or PBS intraperitoneal injection. Scale bar = 50 μm. **B** Representative CD68 staining in the lungs of the four groups and quantitative analysis. **C** ELISA analysis of TNF-α, IL-6, and IL-1β in LPS-challenged RNF99$^{+/+}$ and RNF99$^{-/-}$ mice sera ($n = 8$). **D** Survival of RNF99$^{+/+}$ and RNF99$^{-/-}$ mice following LPS intraperitoneal injection. Sex- and age-matched RNF99$^{+/+}$ and RNF99$^{-/-}$ mice were administered DSS, in drinking water for seven days, or H_2O as a control ($n = 8$–10). **E** Body weight, (**F**) Stool softness, and (**G**) bleeding changes, were measured daily. **H**, **I** Colon lengths of RNF99$^{+/+}$ and RNF99$^{-/-}$ mice were photographed and measured on day 7. **J**, **K** Histopathological changes were observed after H&E staining of colon tissue. Scale bar = 50 μm. **L** ELISA analysis of TNF-α, IL-6, and IL-1β levels in DSS-treated mice sera ($n = 8$). Data were presented as the mean ± SEM and Gaussian distributions were evaluated by the Shapiro–Wilk method. The Mann–Whitney test was used for Fig. 2A and L(IL-1β). The Student's *t* test was used for Fig. 2B, C, K, and L (TNF-α and IL-6). The log-rank (Mantel–Cox) test was used for Fig. 2D. Two-way ANOVA followed by Tukey's post hoc test was used for Fig. 2E–G, I. $^*P < 0.05$, $^{**}P < 0.01$, $^{***}P < 0.001$. Adjusted *P* values are provided for multiple group comparisons.

RNF99 overexpression negatively regulated TLR-mediated inflammatory cytokine production and signaling pathway activation in macrophages

RNF99, as a member of the TRIM family, has a Ring, Coiled-Coil, B-box, and Filamin domains, among which the Ring domain is the key to its E3 ubiquitin ligase function. To further clarify the role of RNF99 in TLR-mediated inflammatory cytokine production, we constructed adenovirus-containing plasmids expressing wild-type RNF99 (RNF99-WT), mutants with deletion of the Ring domain (△-Ring), and a point mutation (C94/97 A). Both △-Ring and C94/97 A mutants lost their E3 ubiquitin ligase function (Supplementary Fig. 4). After RNF99-WT, △-Ring, and C94/97 A were overexpressed in mouse PMs by adenovirus infection and following LPS treatment, it was found that overexpression of RNF99 significantly alleviated TLR-mediated inflammatory factor synthesis (Fig. 5A) and secretion (Fig. 5B), and activation of NF-κB and MAPKs signaling (Fig. 5D–F). Overexpression △-Ring and C94/97 A did not have such effects, suggesting an essential role for the E3 ligase activity of RNF99. Consistent with PMs, the same phenomenon was observed in HEK293-TLR4 overexpressing cell lines (293-TLR4) following LPS treatment (Fig. 5C, Supplementary Fig. 5). These results further indicated that RNF99 can negatively regulate TLR-mediated inflammatory cytokine production and that this effect is closely related to its E3 ubiquitin ligase function.

RNF99 affects the formation of the TAK1-TAB1-TAB2 complex by promoting TAB2 degradation

To elucidate the regulatory mechanisms of RNF99 on TLR-induced proinflammatory cytokine production and activation of the NF-κB and MAPK signaling pathways, we aimed to identify the target molecules of RNF99 in TLR-mediated signaling pathways. We co-transfected several related plasmids IKK-α, IKK-β, IKK-γ, IRAK-1, IRAK-4, TRAF6, TAK1, TAB1, TAB2, with RNF99 into 293-TLR4 cell lines and treated them with LPS. RNF99 overexpression significantly reduced the protein level of TAB2, but had no effect on the expression of other junction proteins (Fig. 6A). Similarly, after LPS stimulation of RNF99$^{+/+}$ and RNF99$^{-/-}$ mouse PMs, only TAB2 expression increased, while the expression of other conjunctions did not change (Fig. 6B). These results indicated that TAB2 may be a target for RNF99 in the TLRs pathway. To further clarify the effect of RNF99 on the expression of TAB2, 293-TLR4 cells were co-transfected with TAB1 or TAB2 with a gradient overexpression of RNF99. It was found that, as the overexpression of RNF99 increased, TAB2 showed a corresponding gradient decrease (Fig. 6D), while the expression of TAB1 did not change (Fig. 6C). However, when △-Ring and C94/97 A mutants of RNF99 were co-transfected with TAB2 in LPS-induced 293-TLR4 cells, the degradation effect was abolished, indicating that the degradation of TAB2 by RNF99 depended on its E3 ubiquitin ligase function (Fig. 6E). To further investigate how RNF99 downregulates TAB2, we employed proteasomal degradation (MG132 and bortezomib) and lysosomal degradation (chloroquine and NH_4Cl) inhibitors. Similarly, TAB2 and RNF99 were co-transfected into LPS-induced 293-TLR4 cells. Degradation of TAB2 by RNF99 disappeared after MG132 or bortezomib treatment. However, such degradation did not change after chloroquine or NH_4Cl treatment in LPS-induced 293-TLR4 cells (Fig. 6F, G). These results indicated that the degradation of TAB2 by RNF99 relies on the proteasomal pathway.

The TAK1-TABs complex is essential for TLR-mediated signal transduction, and TAB2 plays a crucial role in this process [13]. We further explored the effect of RNF99 on the TAK-TABs complex and found that followed by TAB2 increase in RNF99$^{-/-}$ mouse PMs, LPS-induced phosphorylation of TAK was significantly enhanced (Fig. 6H). Meanwhile, the binding of TAK1 and TAB1 significantly increased after RNF99 was knocked out (Fig. 6I). These results confirmed that RNF99 affected the formation of the TAK-TAB complex.

To further confirm the role of TAB2 in RNF99-mediated inflammatory responses, we applied CRISPR-Cas9 system to generate TAB2-deficient RAWs, followed by RNF99 interfered with si-RNA and LPS stimulation. As shown in Supplementary Fig. 6, deficiency of RNF99 on TAB2 knockout background have no effect on the LPS-induced hyper-inflammatory state of macrophages, which further proved that the hyper-inflammatory effect of RNF99$^{-/-}$ is solely mediated by TAB2 stabilization.

RNF99 interacts with TAB2

As a part of the regulatory mechanism, we further confirmed the target molecules of RNF99 in the TLR signaling pathway. First, we co-transfected the TLR signaling pathway junction plasmids IKK-α, IKK-β, IKK-γ, IRAK-1, IRAK-4, TRAF6, TAK1, TAB1, TAB2, with RNF99 into 293-TLR4 cells following LPS treatment. Co-Immunoprecipitation (CO-IP) and immunoblotting results revealed that RNF99 bound to TAB1, TAB2, TAK1, and TRAF6 (Fig. 7A). Our results showed that RNF99 specifically mediated degradation of TAB2, suggesting that TAB2 may be the direct target for RNF99 and that other proteins may be part of the complex involved in signal transduction. We further confirmed the binding of RNF99 and TAB2 by CO-IP separately in 293-TLR4 cells (Fig. 7B). In addition, RNF99 and TAB2 plasmids were constructed on PCDNA3.1-GFP and PCDNA3.1-Flag containing T7 promoters, respectively, and translated in vitro using Promega's TNT in vitro transcription and translation system. Follow-up CO-IP experiments confirmed the direct binding of RNF99 to TAB2 (Fig. 7C). Additionally, the interaction between RNF99 and TAB2 was confirmed by endogenous CO-IP detection in the PMs (Fig. 7D). After overexpression of RNF99 and TAB2 in 293-TLR4 cells, cellular immunofluorescence staining was performed, and confocal laser microscopy revealed that RNF99 and TAB2 had obvious co-localization in the cells (Fig. 7E). All the preceding data indicated intimate interaction between RNF99 and TAB2.

To establish which portions of RNF99 were responsible for the interaction, we generated a series of truncation mutants

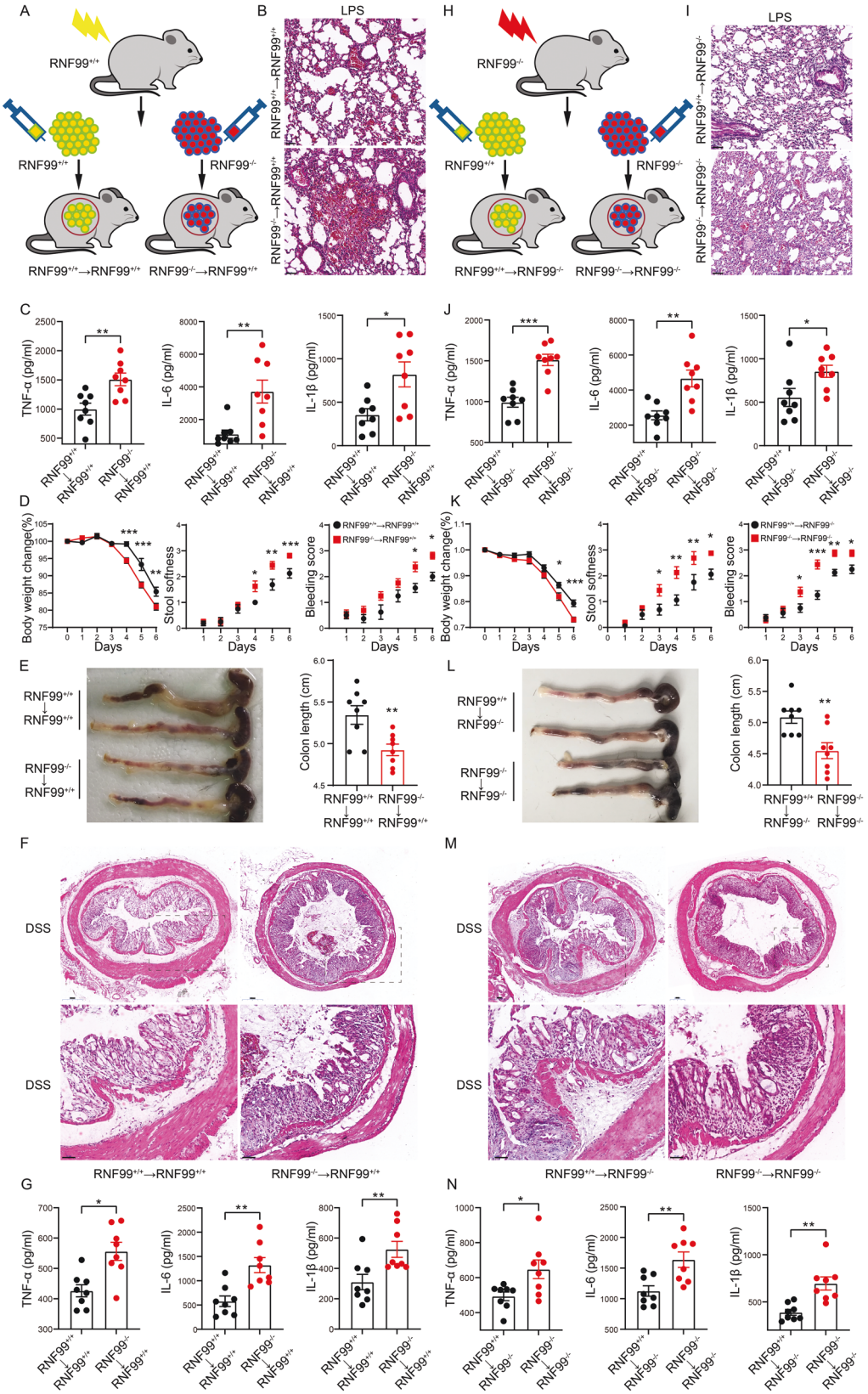

according to the protein structure (Fig. 7F). Through CO-IP experiments in 293-TLR4 cells with LPS stimulation, we found that TAB2 could not interact with the N-terminus and mutants without coiled-coil (△CC) (Fig. 7G). This indicated that the Coiled-coil in RNF99 is the structural domain that combined with TAB2. Together, our findings suggested that TAB2 is a target molecule of RNF99 in the TLRs signaling pathway.

Fig. 3 Regulation of TLRs-mediated inflammatory diseases by RNF99 in macrophages. Sex- and age-matched RNF99$^{+/+}$ and RNF99$^{-/-}$ mouse bone marrow cells were depleted by irradiating. Irradiated mice were transplanted bone marrow cells from RNF99$^{+/+}$ or RNF99$^{-/-}$ mice donors, respectively. Intraperitoneal injection of LPS was performed to construct an endotoxemia mouse model after bone marrow reconstruction. **A** Schematic diagram of bone marrow-transplantation (RNF99$^{+/+}$ → RNF99$^{+/+}$ and RNF99$^{-/-}$ → RNF99$^{+/+}$). **B** H&E staining of lung sections from LPS-induced RNF99$^{+/+}$ mice treated with bone marrow cells from RNF99$^{+/+}$ or RNF99$^{-/-}$ mice. Scale bar = 50 μm. **C** ELISA analysis of TNF-α, IL-6, and IL-1β levels in LPS-treated mice sera ($n = 8$). DSS was used to construct a mouse model of acute colitis following bone marrow reconstruction. **D** Clinical and pathological changes in DSS-induced RNF99$^{+/+}$ mice transplanted with bone marrow cells from RNF99$^{+/+}$ or RNF99$^{-/-}$. **E** Changes in colon length in DSS-induced colitis mice. **F** Histopathological changes in the colon of DSS-induced mice. Scale bar = 50 μm. **G** ELISA analysis of TNF-α, IL-6, and IL-1β levels in DSS-treated mice sera ($n = 8$). **H** Schematic diagram of bone marrow-transplantation (RNF99$^{+/+}$ → RNF99$^{-/-}$ and RNF99$^{-/-}$ → RNF99$^{-/-}$). **I** H&E staining of lung sections from LPS-induced RNF99$^{-/-}$ mice treated with bone marrow cells from RNF99$^{+/+}$ or RNF99$^{-/-}$ mice. Scale bar = 50 μm. **J** ELISA analysis of TNF-α, IL-6, and IL-1β levels in LPS-treated mice sera ($n = 8$). **K** Clinical and pathological changes in DSS-induced RNF99$^{-/-}$ mice transplanted with bone marrow cells from RNF99$^{+/+}$ or RNF99$^{-/-}$. **L** Changes in colon length in DSS-induced colitis mice. **M** Histopathological changes in the colon of DSS-induced mice. Scale bar = 50 μm. **N** ELISA analysis of TNF-α, IL-6, and IL-1β levels in DSS-treated mice sera ($n = 8$). Data were presented as the mean ± SEM and Gaussian distributions were evaluated by the Shapiro–Wilk method. The Student's *t* test was used for Fig. 3C (TNF-α and IL-1β), **E**, **G** (TNF-α and IL-6), (**J**, **L**, **N**). The Mann–Whitney test was used for Fig. 3C (IL-6) and G (IL-1β). Two-way analysis of variance (ANOVA) followed by Tukey's post-hoc test was used for Fig. 3D. The Student's *t* test was used for Fig. 3I, J. $^{*}P < 0.05$, $^{**}P < 0.01$, $^{***}P < 0.001$. Adjusted *P* values are provided for multiple group comparisons.

RNF99 targets K611 of TAB2 for K48-linked polyubiquitination

Protein ubiquitination is closely associated with the ubiquitin-proteasomal degradation pathway [33, 34]. After demonstrating that RNF99 mediates the degradation of TAB2 via proteasomal pathway and that this degradation depends on E3 ubiquitin ligase activity, we further explored whether RNF99 can mediate ubiquitin modification of TAB2. HA-labeled ubiquitin, Myc-RNF99, and Flag-TAB2 overexpression plasmids were co-transfected into the 293-TLR4 cell line. It was found that RNF99 significantly promoted the ubiquitination level of TAB2 (Fig. 8A, Supplementary Fig. 7A). The HA-ubiquitin and GFP-TAB2 overexpression plasmids were co-transfected with plasmids of Flag-RNF99-WT, △Ring, or C94/C97A in 293-TLR4 cells with LPS treatment. The results showed that RNF99-WT could promote the ubiquitination of TAB2, but not RNF99-△Ring and RNF99-C94/C97A (Fig. 8B). These results suggested that RNF99 can promote ubiquitin modification of TAB2 and that this effect is closely related to the E3 ubiquitin ligase function of RNF99.

The full-length ubiquitin molecule contains seven lysine sites (K6, K11, K27, K29, K33, K48, and K63). K48- and K63-linked ubiquitination are the two most studied types of ubiquitination, and K48-linked ubiquitination is often reported to involve proteasomal degradation [35, 36]. To further explore the ubiquitin modification effects of RNF99 on TAB2, we co-transfected Myc-RNF99 and Flag-TAB2 with various types of ubiquitin (WT, K48, and K63) in LPS-treated 293-TLR4 cells. The results showed that RNF99 could significantly promote K48-linked ubiquitination of TAB2 but had no effect on the K63-linked ubiquitination (Fig. 8C). Consistently, co-transfection of K48-ubiquintin and TAB2 with RNF99 mutants (△Ring, C94/C97A) in LPS-treated 293-TLR4 cells revealed that RNF99 without E3 ubiquitin ligase function did not affect the K48-linked ubiquitination level of TAB2 (Fig. 8D). After stimulation of PMs from RNF99$^{+/+}$ and RNF99$^{-/-}$ mice with LPS, tandem ubiquitin-binding entities (TUBEs) pull-down assays were performed to purify the ubiquitinated substrates, detection showed that endogenous K48-linked ubiquitination of TAB2 was decreased in PMs from RNF99$^{-/-}$ mice upon LPS treatment (Fig. 8E).

To further explore the mechanism of ubiquitin modification of TAB2 by RNF99 in vitro, Promega's TNT in vitro transcription and translation system was used to translate GFP-RNF99 and Flag-TAB2, GST-TRIM31 served as a negative control. The translated protein was then added to BostonBiochem's in vitro ubiquitin modification system in the presence of E1, UbcH5a, ubiquitin (WT), K63 (containing only K63 lysine)-ubiquitin, and K48-ubiquitin (containing only K48 lysine). TAB2 was ubiquitinated by RNF99 in the presence of WT- and K48-ubiquitin but not by K63-ubiquitin (Fig. 8F). Taken together, these results confirmed the critical role of RNF99 in K48-linked ubiquitination of TAB2.

Previous omics research on TAB2 ubiquitination predicted that lysine 522, 611, 653, and 656 of TAB2 were ubiquitinated [37–39]. However, an E3 ligase that regulates ubiquitination at these sites has not yet been identified. To clarify which lysine site on TAB2 is responsible for ubiquitination by RNF99, we constructed over-expression plasmids with mutations in different lysine sites of TAB2 (K522R, K611R, K653R, K656R, and K653/656 R). After co-transfection of the TAB2 mutants with Myc-RNF99 and ubiquitin in 293-TLR4 cells, it was found that RNF99 lost the ubiquitination function in the K611R mutant (containing all lysine except the 611 lysine that was mutated), indicating that K611 is the site of ubiquitination modification of TAB2 by RNF99 (Fig. 8G). In addition, after K611 in TAB2 was mutated, the degradation effect of RNF99 on TAB2 disappeared (Fig. 8H, Supplementary Fig. 7B). The ubiquitination lysine site was consistent with the degradation site of TAB2 by RNF99. Overall, these results suggested that RNF99 promotes proteasomal degradation by modifying lysine 611 of TAB2 through ubiquitination and plays an essential role in inhibiting NF-κB and MAPK signaling pathways and the innate immune response.

DISCUSSION

The induction of innate immune response is the first line of defense against pathogen invasion [1]. The TLRs signaling excessive activation in macrophages is an important cause of inflammatory lesions such as sepsis and colitis [2, 5, 6]. Ubiquitination plays a key role in TLR-mediated inflammatory diseases and that many E3 ubiquitin ligases are involved. For example, the E3 ligase TRIM26 positively regulates DSS-induced colitis and LPS-induced lung injury by modifying TAB1 via ubiquitination [40]. The E3 ligase TRIM31 promotes DSS-induced colitis by promoting NLRP3 ubiquitination and proteasomal degradation [41]. Previous studies on RNF99 have mainly focused on biological processes involved in tumor progression [22, 42]. However, the cognition of RNF99's role in macrophage-mediated inflammatory immune response is still limited.

Here, we found that RNF99 expression was reduced in G^{-} infected peripheral blood monocytes and macrophages with TLRs ligands treatment. These results suggested that RNF99 may be involved in a feedback process in the TLR-mediated innate immune response and the body's resistance to bacterial infection, and RNF99 may also be a promising diagnostic biomarker. Accordingly, in vivo research revealed that RNF99 deficiency markedly increased LPS-induced endotoxemia and

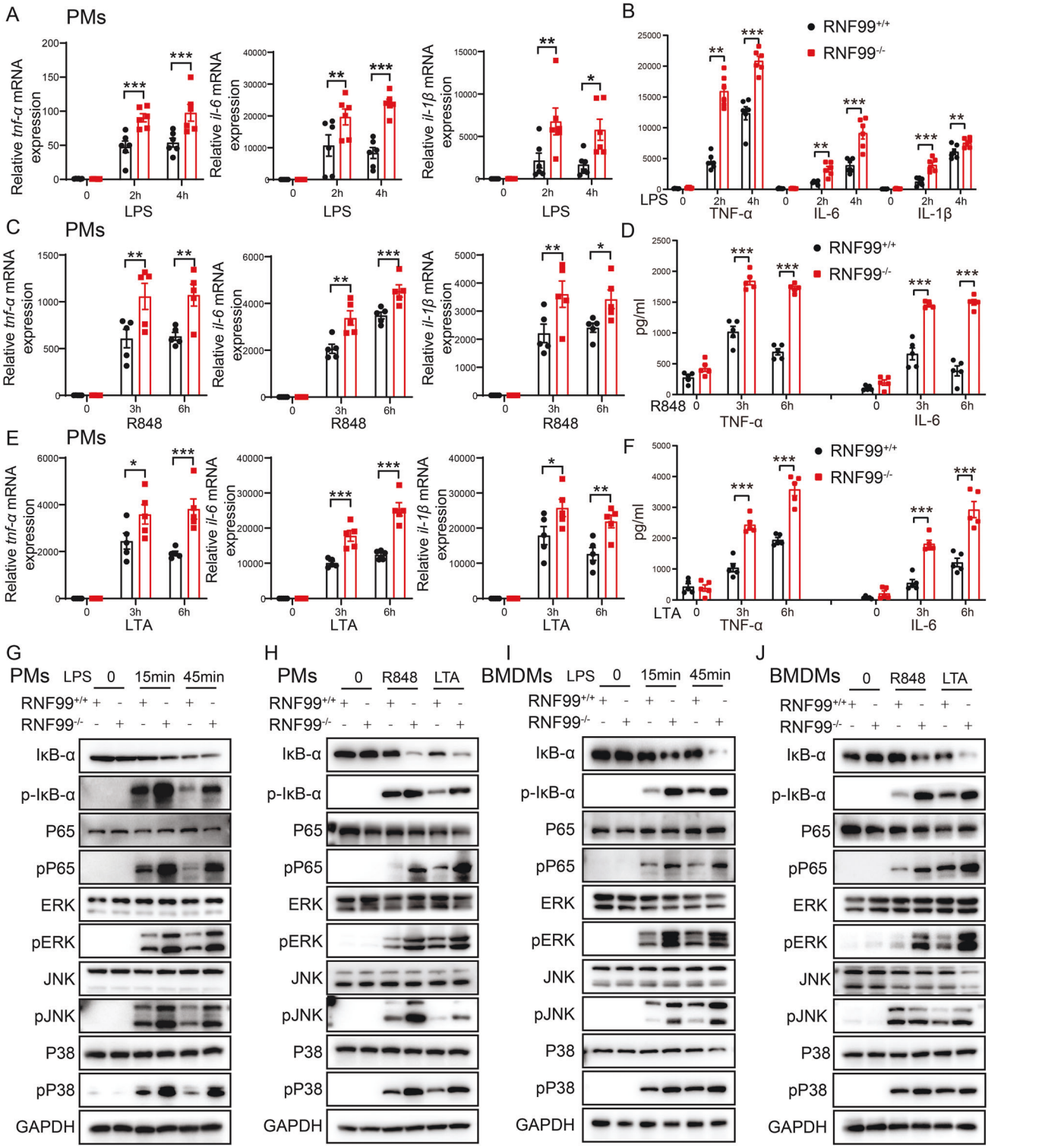

Fig. 4 RNF99 deficiency positively regulated TLRs-mediated inflammatory cytokine production and signaling pathway activation in macrophages. A, **B** RT-PCR and ELISA analysis of TNF-α, IL-6, and IL-1β in PMs, from RNF99$^{+/+}$ or RNF99$^{-/-}$ mice or supernatants of PMs stimulated by LPS (100 ng/ml) for indicated hours ($n = 6$). **C**, **D** RT-PCR and ELISA analysis of TNF-α, IL-6, and IL-1β in PMs from RNF99$^{+/+}$ or RNF99$^{-/-}$ mice or supernatants of PMs stimulated by R848 (10 ng/ml) for indicated hours ($n = 6$). **E**, **F** RT-PCR and ELISA analysis of TNF-α, IL-6, and IL-1β in PMs from RNF99$^{+/+}$ or RNF99$^{-/-}$ mice or supernatants of PMs stimulated by LTA (10 ng/ml) for indicated hours ($n = 6$). **G**, **H** Immunoblot analysis of phosphorylation levels of IκB-α, P65, ERK, JNK, and P38 in PMs, from RNF99$^{+/+}$ or RNF99$^{-/-}$ mice, stimulated by LPS for indicated hours; R848 and LTA stimulation was for 30 min. **I**, **J** Immunoblot analysis of phosphorylation levels of IκB-α, P65, ERK, JNK, and P38 in BMDMs, from RNF99$^{+/+}$ or RNF99$^{-/-}$ mice, stimulated by LPS for indicated hours; R848 and LTA stimulation was for 30 min. Data were presented as the mean ± SEM and Gaussian distributions were evaluated by the Shapiro–Wilk method. Two-way ANOVA followed by Tukey post hoc test was used for Fig. 4A–F. *$P < 0.05$, **$P < 0.01$, ***$P < 0.001$. Adjusted P values are provided for multiple group comparisons.

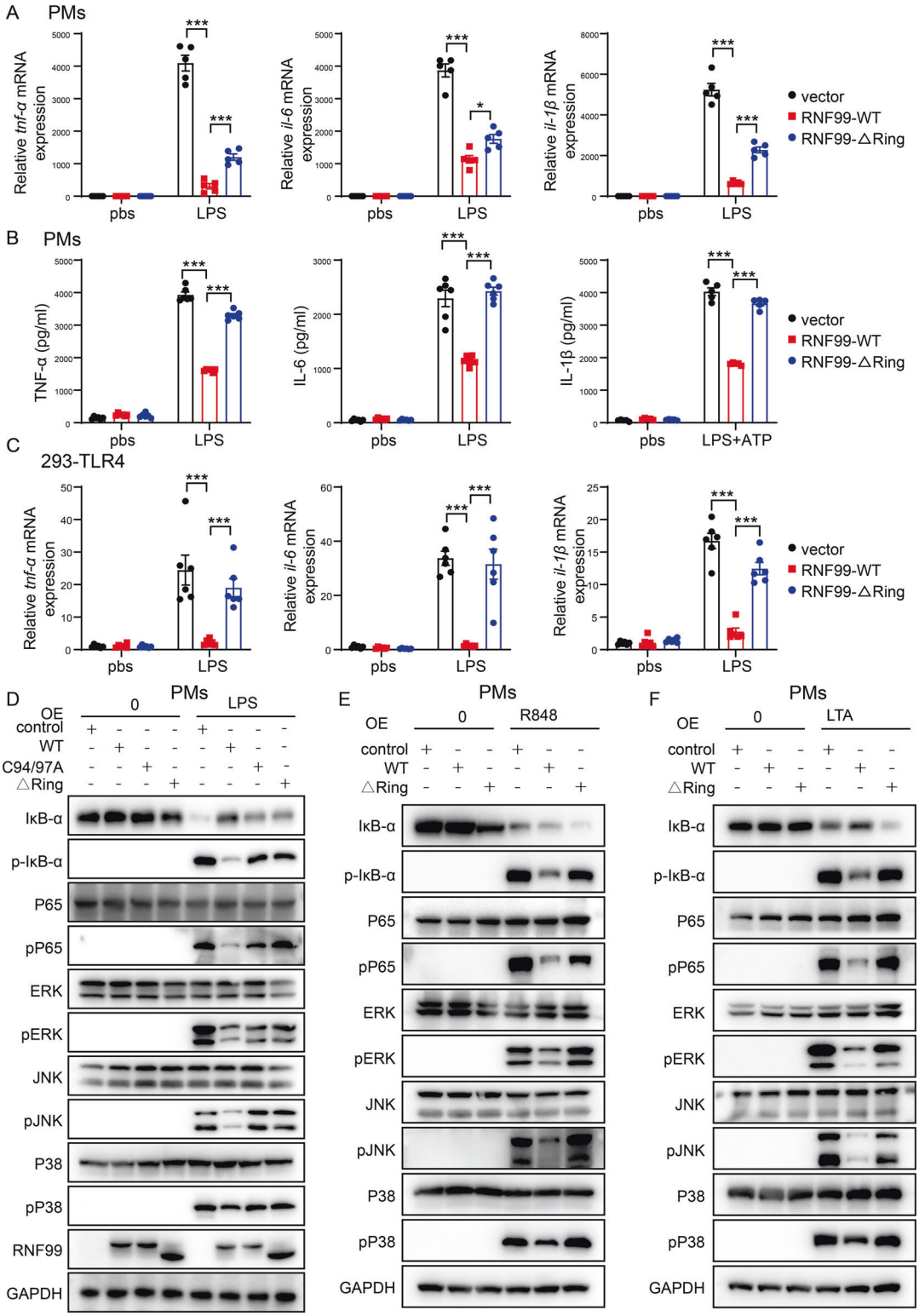

Fig. 5 RNF99 overexpression negatively regulates TLRs-mediated inflammatory cytokine production and signaling pathway activation in macrophages. A, **B** RT-PCR and ELISA analysis of TNF-α, IL-6, and IL-1β in PMs with adenovirus (vector, RNF99-WT or RNF99-△Ring) overexpression and LPS stimulation for 4 h ($n = 5–6$). **C** RT-PCR analysis of *tnf-α*, *il-6*, and *il-1β* in 293-TLR4 cells with adenovirus (vector, RNF99-WT or RNF99-△Ring) overexpression and LPS stimulation for 4 h ($n = 6$). **D** Immunoblot analysis of phosphorylation levels of IκB-α, P65, ERK, JNK, and P38 in PMs with adenovirus (vector, RNF99-WT, RNF99-△Ring, and RNF99-C94/97 A) overexpression and LPS stimulation for 30 min. **E** Immunoblot analysis of phosphorylation levels of IκB-α, P65, ERK, JNK, and P38 in PMs with adenovirus (vector, RNF99-WT or RNF99-△Ring) overexpression and R848 stimulation for 30 min. **F** Immunoblot analysis of phosphorylation levels of IκB-α, P65, ERK, JNK, and P38 in PMs with adenovirus (vector, RNF99-WT or RNF99-△Ring) overexpression and LTA stimulation for 30 min. Data were presented as the mean ± SEM and Gaussian distributions were evaluated by the Shapiro–Wilk method. Two-way ANOVA followed by Tukey post hoc test was used for Fig. 5. $^{*}P < 0.05$, $^{**}P < 0.01$, $^{***}P < 0.001$. Adjusted *P* values are provided for multiple group comparisons.

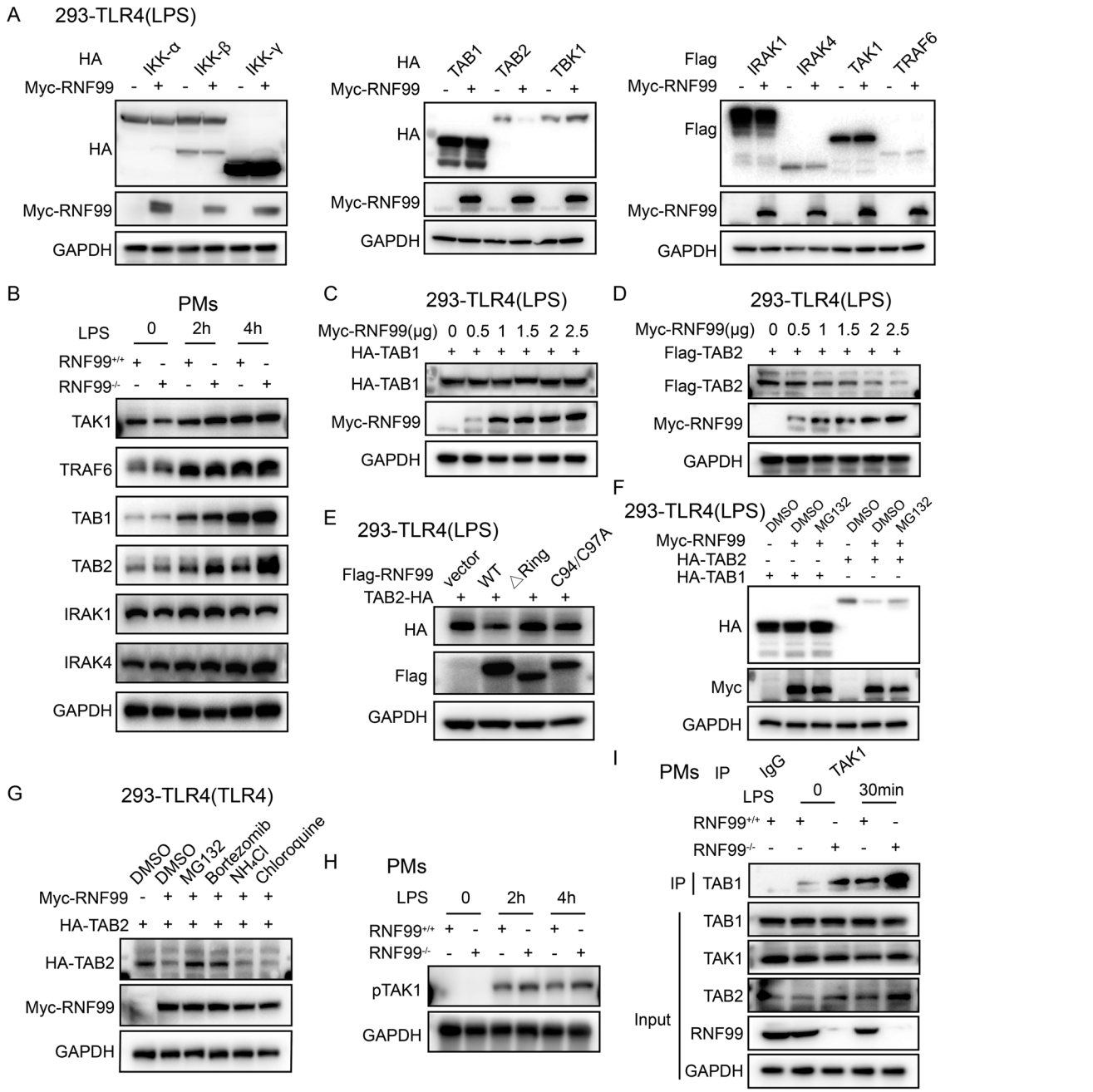

Fig. 6 RNF99 affects the formation of the TAK1-TAB1-TAB2 complex via promoting TAB2 degradation. A Representative immunoblot images of HA-tagged IKK-α, IKK-β, IKK-γ, TAB1, TAB2, TBK1, Flag-tagged IRAK-1, IRAK-4, TRAF6, and TAK1 in LPS-treated 293-TLR4 cells transfected with vector or Myc-RNF99. **B** Representative Immunoblot images of TAK1, TRAF6, TAB1, TAB2, IRAK-1, and IRAK-4 in PMs, from $RNF99^{+/+}$ or $RNF99^{-/-}$ mice, stimulated by LPS for indicated hours. **C**, **D** Representative Immunoblot images of HA-TAB1 and Flag-TAB2 in LPS-treated 293-TLR4 cells transfected with a concentration gradient of Myc-RNF99. **E** Representative immunoblot images of HA-TAB2 in LPS-treated 293-TLR4 cells transfected with vector or Myc-RNF99 (WT, Ring, and C94/97 A). **F** Representative immunoblot images of HA-TAB1 and HA-TAB2 in LPS-treated 293-TLR4 cells transfected with Myc-RNF99 and pretreated with MG132. **G** Representative Immunoblot images of HA-TAB2 in LPS-treated 293-TLR4 cells transfected with Myc-RNF99 and pretreated with DMSO, MG132, Bortezomib, NH_4Cl, and chloroquine. **H** Representative Immunoblot images of pTAK1 in PMs, from $RNF99^{+/+}$ or $RNF99^{-/-}$ mice, stimulated by LPS for indicated hours. **I** Co-IP assay of TAB1 changes in LPS-treated $RNF99^{+/+}$ or $RNF99^{-/-}$ mice PMs with TAK1.

DSS-induced colitis in mice. From bone marrow-transplant experiments, we confirmed that RNF99 in macrophages plays an important anti-inflammatory role in endotoxemia and colitis. Our results also confirmed that RNF99 knockout promoted the production of inflammatory cytokines in macrophages induced by TLRs ligands. Herein, we report, for the first time, the important role of E3 ligase RNF99 in macrophage function and the innate immune inflammatory response. Our study indicated that the decreased RNF99 expression, induced by pathogenic microorganisms in the late stage of infection, may be responsible for the excessive inflammatory response in the body, therefore, the development of agonists targeting RNF99 may be an important strategy to improve endotoxemia and refractory colitis in the future.

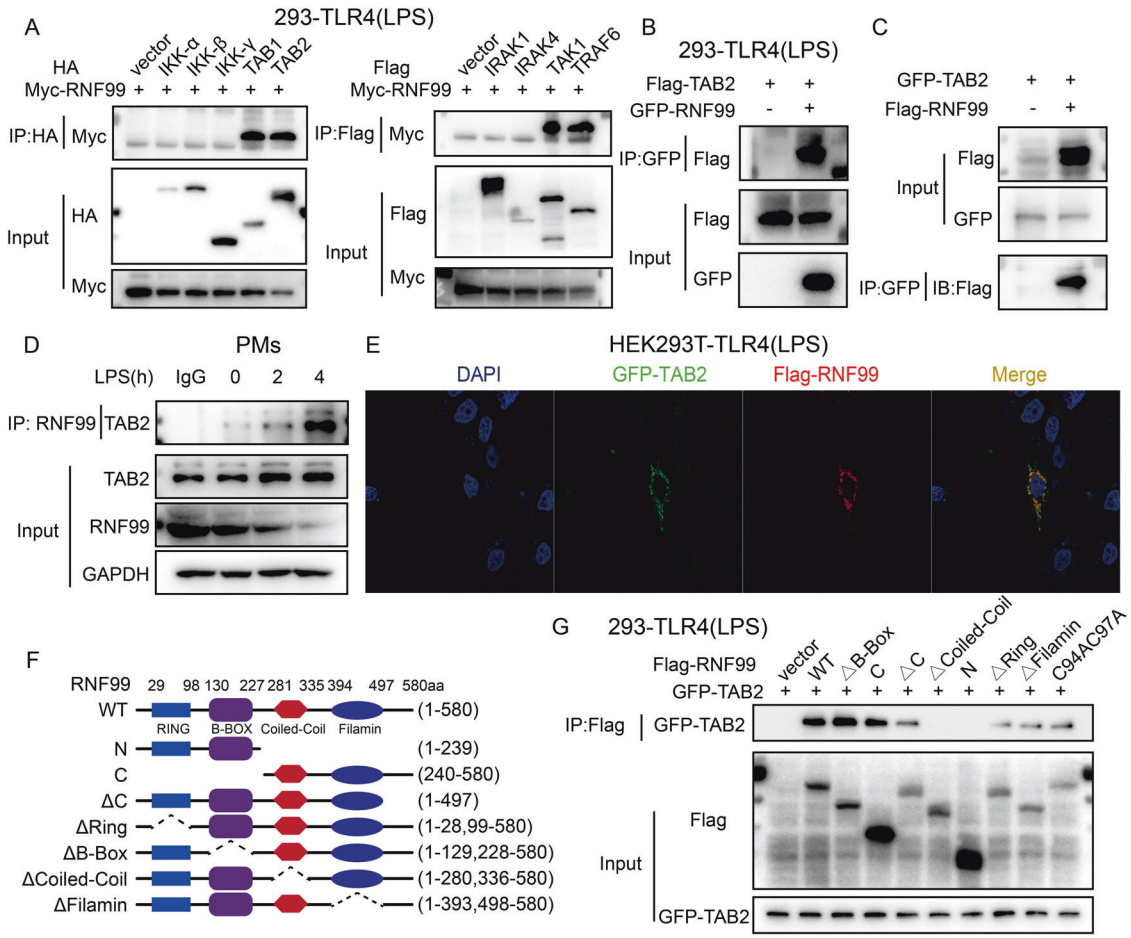

Fig. 7 RNF99 interacts with TAB2. **A** CO-IP analysis of interactors with Myc-RNF99 in LPS-treated 293-TLR4 cells. **B** CO-IP analysis of the interaction between Flag-TAB2 and GFP-RNF99 in LPS-treated 293-TLR4 cells. **C** In vitro CO-IP analysis of the interaction between GFP-TAB2 and Flag-RNF99 expressed in TNT transcription and translation system. **D** CO-IP analysis of the interaction between TAB2 and RNF99 in PMs with LPS-treated. **E** Representative confocal laser microscopic images of the colocalization of GFP-TAB2 and Flag-RNF99 in LPS-treated 293-TLR4 cells. **F** Schematic representations of human RNF99 (WT) and its truncated mutants. **G** CO-IP analysis of the interactions between RNF99 mutants with GFP-TAB2 in LPS-treated 293-TLR4 cells.

TLRs are important pattern recognition receptors on macrophages, which recognize surface pathogenic bacterial molecules, such as lipopolysaccharides, and then induce signal transduction and inflammatory cytokine production [3, 4]. The protein kinase TAK1 phosphorylates downstream MAPKs and IKKs, it completes the activation of signal transduction and induces the production of TNFα, IL-6, IL-1β, and other cytokines [4]. Previous studies have shown that TAB1 forms a complex with TAK1 and promotes phosphokinase activation of TAK1 [13]. TAB2 is also a key regulatory molecule for the formation of this complex. Several studies have shown that TAB2 degradation or deficiency can effectively inhibit TAK1 kinase activation and the related inflammatory responses [24]. Ubiquitination is an important mechanism to regulate protein degradation and stability [43]. It has been reported that TRIM27 is a key regulator of hepatic I/R injury by mediating lysosomal degradation of TAB2/3 and suppression of downstream TAK1-JNK/p38 signaling [44]. RNF4, TRIM38, and TRIM22 also regulate NF-κB activation through TAB2 lysosomal degradation [26, 28, 29]. To date, there are still many questions regarding TAB2 ubiquitination modification and degradation. First, TRIM family members that regulate ubiquitination and proteasomal degradation of TAB2 have not yet been reported. Second, the key lysine sites on TAB2 that regulate lysosomal and proteasomal degradation remain unknown.

Using macrophages and HEK293-TLR4 cell lines as cell models, we found that E3 ligase RNF99 can bind to TAB2 and promote its K48 ubiquitination modification and proteasomal degradation, which further inhibits TAK1/TABs complex formation and TAK1 kinase activation. Immunoprecipitation assays on the HEK293-TLR4 cell line showed that RNF99 binds to TAB2, TAK1, and TAB1. This may be because TAK1/TAB1/TAB2 form a complex in mammalian cells and RNF99 binds to TAB2 and precipitates TAK1 and TAB1 together. Our data further showed that the effect of RNF99 overexpression or knockout on TAB2 protein was specific. The direct effect of RNF99 on TAB2 binding and ubiquitination was further elucidated using the following in vitro experiments: protein translation system, protein immunoprecipitation assay, and protein ubiquitination assay. Previous omics studies on TAB2 ubiquitination have shown that lysine positions K522, K611, K653, and K656 on TAB2 protein could undergo ubiquitination, but the corresponding E3 ligase has not been identified. We constructed overexpression plasmids with mutations in different lysine sites of TAB2 and identified that K611 could be ubiquitinated by RNF99, leading to the degradation of TAB2 via the proteasome pathway.

In summary, we demonstrated that RNF99 was a key regulator of the TLR signaling pathway. By promoting K48-linked polyubiquitination of TAB2 at K611 and proteasomal degradation of TAB2, RNF99

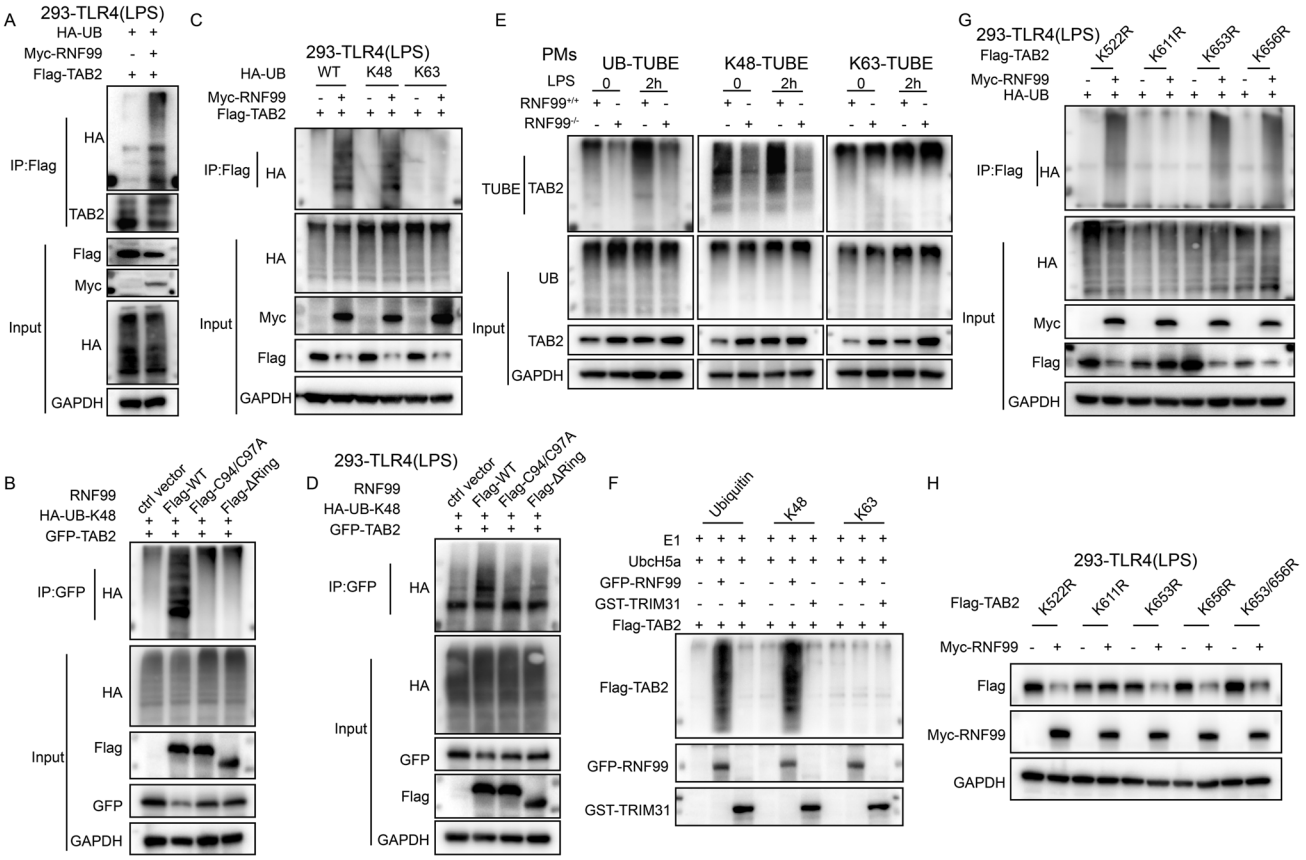

Fig. 8 RNF99 targets K611 of TAB2 for K48-linked polyubiquitination. A CO-IP analysis of Flag-TAB2 ubiquitination in LPS-treated 293-TLR4 cells transfected with Myc-RNF99 and HA-ubiquitin (UB). **B** CO-IP analysis of GFP-TAB2 ubiquitination in LPS-treated 293-TLR4 cells transfected with HA-UB, as well as vector or plasmid encoding Flag-RNF99 (WT), Flag-RNF99-ΔRing or Flag-RNF99 (C53A/C56A). **C** CO-IP analysis of TAB2 ubiquitination in LPS-treated 293-TLR4 cells transfected with different UB (WT, K48, or K63), as well as Myc-RNF99 (WT), and Flag-TAB2 plasmids. **D** CO-IP analysis of GFP-TAB2 ubiquitination in LPS-treated 293-TLR4 cells transfected with HA-UB-K48, as well as Flag-RNF99 (WT), Flag-RNF99-ΔRing or Flag-RNF99 (C53A/C56A) plasmids. **E** Co-IP analysis of TAB2 ubiquitination after ubiquitin (TUBE) pull-downs in PMs from $RNF99^{+/+}$ or $RNF99^{-/-}$ mice, stimulated by LPS for 2 h. **F** In vitro ubiquitination analysis of TAB2 with TNT system translated GFP-RNF99, GST-TRIM31 and Flag-TAB2 in the presence of ubiquitin (WT, K48 or K63), E1, and UbcH5a. **G** CO-IP analysis of Flag-TAB2 ubiquitination in LPS-treated 293-TLR4 cells transfected with HA-UB, Myc-RNF99, as well as Flag-TAB2 point mutants (K522R, K611R, K653R and K656R) plasmids. **H** Representative immunoblot images of Flag-TAB2 point mutants (K522R, K611R, K653R, K656R, K653/656R) in LPS-treated 293-TLR4 cells transfected with vector or Myc-RNF99 plasmid.

inhibited the formation of the TAK-TABs complex and the activation of downstream NF-κB and MAPKs signaling pathways, thereby downregulating the production of proinflammatory factors (Supplementary Fig. 8). Our study demonstrated, for the first time, that RNF99 may be a promising diagnostic biomarker and therapeutic target for the treatment of TLR-related inflammatory diseases.

DATA AVAILABILITY

The datasets are available from the corresponding author on reasonable request.

REFERENCES

1. Medzhitov R. Recognition of microorganisms and activation of the immune response. Nature. 2007;449:819–26.
2. Fitzgerald KA, Kagan JC. Toll-like receptors and the control of immunity. Cell. 2020;180:1044–66.
3. Kawai T, Akira S. Toll-like receptors and their crosstalk with other innate receptors in infection and immunity. Immunity. 2011;34:637–50.
4. Kawai T, Akira S. TLR signaling. Semin Immunol. 2007;19:24–32.
5. Abreu MT, Fukata M, Arditi M. TLR signaling in the gut in health and disease. J Immunol. 2005;174:4453–60.
6. Lu Y, Li X, Liu S, Zhang Y, Zhang D. Toll-like receptors and inflammatory bowel disease. Front Immunol. 2018;9:72.
7. Wang Y, Zhang S, Li H, Wang H, Zhang T, Hutchinson MR, et al. Small-molecule modulators of toll-like receptors. Acc Chem Res. 2020;53:1046–55.
8. Tse K, Horner AA. Update on toll-like receptor-directed therapies for human disease. Ann Rheum Dis. 2007;66:iii77–80.
9. Pfalzgraff A, Weindl G. Intracellular lipopolysaccharide sensing as a potential therapeutic target for sepsis. Trends Pharm Sci. 2019;40:187–97.
10. Schön MP, Schön M. TLR7 and TLR8 as targets in cancer therapy. Oncogene. 2008;27:190–9.
11. Kang SS, Sim JR, Yun CH, Han SH. Lipoteichoic acids as a major virulence factor causing inflammatory responses via Toll-like receptor 2. Arch pharmacal Res. 2016;39:1519–29.
12. Totzke J, Scarneo SA, Yang KW, Haystead TAJ. TAK1: a potent tumour necrosis factor inhibitor for the treatment of inflammatory diseases. Open Biol. 2020;10:200099.
13. Xu YR, Lei CQ. TAK1-TABs complex: a central signalosome in inflammatory responses. Front Immunol. 2020;11:608976.
14. Roh YS, Song J, Seki E. TAK1 regulates hepatic cell survival and carcinogenesis. J Gastroenterol. 2014;49:185–94.
15. Mihaly SR, Ninomiya-Tsuji J, Morioka S. TAK1 control of cell death. Cell death Differ. 2014;21:1667–76.
16. Beck DB, Werner A, Kastner DL, Aksentijevich I. Disorders of ubiquitylation: unchained inflammation. Nat Rev Rheumatol. 2022;18:435–47.
17. Zhang X, Smits AH, van Tilburg GB, Jansen PW, Makowski MM, Ovaa H, et al. An interaction landscape of ubiquitin signaling. Mol Cell. 2017;65:941–55. e948

18. Wang C, Chen T, Zhang J, Yang M, Li N, Xu X, et al. The E3 ubiquitin ligase Nrdp1 'preferentially' promotes TLR-mediated production of type I interferon. Nat Immunol. 2009;10:744–52.
19. Meng Z, Xu R, Xie L, Wu Y, He Q, Gao P, et al. A20/Nrdp1 interaction alters the inflammatory signaling profile by mediating K48- and K63-linked polyubiquitination of effectors MyD88 and TBK1. J Biol Chem. 2021;297:100811.
20. Hu MM, Xie XQ, Yang Q, Liao CY, Ye W, Lin H, et al. TRIM38 negatively regulates TLR3/4-mediated innate immune and inflammatory responses by two sequential and distinct mechanisms. J Immunol. 2015;195:4415–25.
21. Zhao W, Wang L, Zhang M, Wang P, Yuan C, Qi J, et al. Tripartite motif-containing protein 38 negatively regulates TLR3/4- and RIG-I-mediated IFN-beta production and antiviral response by targeting NAP1. J Immunol. 2012;188:5311–8.
22. Zhang J, Zhang C, Cui J, Ou J, Han J, Qin Y, et al. TRIM45 functions as a tumor suppressor in the brain via its E3 ligase activity by stabilizing p53 through K63-linked ubiquitination. Cell Death Dis. 2017;8:e2831.
23. Shibata M, Sato T, Nukiwa R, Ariga T, Hatakeyama S. TRIM45 negatively regulates NF-κB-mediated transcription and suppresses cell proliferation. Biochem Biophys Res Commun. 2012;423:104–9.
24. Hirata, Y, Takahashi, M, Morishita, T, Noguchi, T, Matsuzawa, A post-translational modifications of the TAK1-TAB complex. Int J Mol Sci. 2017;18:205.
25. Braun H, Staal J. Stabilization of the TAK1 adaptor proteins TAB2 and TAB3 is critical for optimal NF-κB activation. FEBS J. 2020;287:3161–4.
26. Hu MM, Yang Q, Zhang J, Liu SM, Zhang Y, Lin H, et al. TRIM38 inhibits TNFalpha- and IL-1beta-triggered NF-kappaB activation by mediating lysosome-dependent degradation of TAB2/3. Proc Natl Acad Sci USA. 2014;111:1509–14.
27. Shi M, Deng W, Bi E, Mao K, Ji Y, Lin G, et al. TRIM30 alpha negatively regulates TLR-mediated NF-kappa B activation by targeting TAB2 and TAB3 for degradation. Nat Immunol. 2008;9:369–77.
28. Qiu H, Huang F, Xiao H, Sun B, Yang R. TRIM22 inhibits the TRAF6-stimulated NF-κB pathway by targeting TAB2 for degradation. Virologica Sin. 2013;28:209–15.
29. Tan B, Mu R, Chang Y, Wang YB, Wu M, Tu HQ, et al. RNF4 negatively regulates NF-κB signaling by down-regulating TAB2. FEBS Lett. 2015;589:2850–8.
30. Blander JM, Longman RS, Iliev ID, Sonnenberg GF, Artis D. Regulation of inflammation by microbiota interactions with the host. Nat Immunol. 2017;18:851–60.
31. Bang B, Lichtenberger LM. Methods of inducing inflammatory bowel disease in mice. Curr Protoc Pharm. 2016;72:5.58.51–55.58.42.
32. Eichele DD, Kharbanda KK. Dextran sodium sulfate colitis murine model: An indispensable tool for advancing our understanding of inflammatory bowel diseases pathogenesis. World J Gastroenterol. 2017;23:6016–29.
33. Varshavsky A. The ubiquitin system, autophagy, and regulated protein degradation. Annu Rev Biochem. 2017;86:123–8.
34. Zientara-Rytter, K. and Subramani, S The roles of ubiquitin-binding protein shuttles in the degradative fate of ubiquitinated proteins in the ubiquitin-proteasome system and autophagy. Cells. 2019;8:40.
35. Tracz M, Bialek W. Beyond K48 and K63: non-canonical protein ubiquitination. Cell Mol Biol Lett. 2021;26:1.
36. Xu P, Duong DM, Seyfried NT, Cheng D, Xie Y, Robert J, et al. Quantitative proteomics reveals the function of unconventional ubiquitin chains in proteasomal degradation. Cell. 2009;137:133–45.
37. Akimov V, Barrio-Hernandez I, Hansen SVF, Hallenborg P, Pedersen AK, Bekker-Jensen DB, et al. UbiSite approach for comprehensive mapping of lysine and N-terminal ubiquitination sites. Nat Struct Mol Biol. 2018;25:631–40.
38. Vogl AM, Phu L, Becerra R, Giusti SA, Verschueren E, Hinkle TB, et al. Global site-specific neddylation profiling reveals that NEDDylated cofilin regulates actin dynamics. Nat Struct Mol Biol. 2020;27:210–20.
39. Rose CM, Isasa M, Ordureau A, Prado MA, Beausoleil SA, Jedrychowski MP, et al. Highly multiplexed quantitative mass spectrometry analysis of ubiquitylomes. Cell Syst. 2016;3:395–403. e394
40. Zhao J, Cai B, Shao Z, Zhang L, Zheng Y, Ma C, et al. TRIM26 positively regulates the inflammatory immune response through K11-linked ubiquitination of TAB1. Cell Death Differ. 2021;28:3077–91.
41. Song H, Liu B, Huai W, Yu Z, Wang W, Zhao J, et al. The E3 ubiquitin ligase TRIM31 attenuates NLRP3 inflammasome activation by promoting proteasomal degradation of NLRP3. Nat Commun. 2016;7:13727.
42. Peng X, Wen Y, Zha L, Zhuang J, Lin L, Li X, et al. TRIM45 suppresses the development of non-small cell lung cancer. Curr Mol Med. 2020;20:299–306.
43. Cockram PE, Kist M, Prakash S, Chen SH, Wertz IE, Vucic D. Ubiquitination in the regulation of inflammatory cell death and cancer. Cell Death Differ. 2021;28:591–605.
44. Chen SY, Zhang HP, Li J, Shi JH, Tang HW, Zhang Y, et al. Tripartite motif-containing 27 attenuates liver ischemia/reperfusion injury by suppressing transforming growth factor β-activated kinase 1 (TAK1) by TAK1 binding protein 2/3 degradation. Hepatology. 2021;73:738–58.

ACKNOWLEDGEMENTS

We thank Dr. Hongwei Pan (Department of Clinical Laboratory, Qilu Hospital of Shandong University, China) for the human samples collection.

AUTHOR CONTRIBUTIONS

MZ, YZ, and CZ designed, supervised the study, and revision and final approval of the manuscript. JZ and LC contributed to data research, analysis, and manuscript writing. AG, LWY, QL, YPL, WQQ, YHH, WHS, and GHS contributed to the data collection and analysis. RQR acquired human samples. All the authors have read the manuscript and provided useful comments.

FUNDING

This work was supported by grants of the National Natural Science Foundation of China (No. 81970373, 31770977, 82270487, 82200502, 81920108003, 82030051 and 82200507), the Postdoctoral Science Foundation of China and Shandong Province (No. 2018M630789, 201901009 and 2021ZLGX02), the Shandong Provincial Natural Science Foundation (No. ZR2020YQ53, 2021ZDSYS05, 2021SFGC0503, ZR2022QH089 and ZR2022QH211), the Program of Introducing Talents of Discipline to Universities (BP0719033), the National Key Research and Development Program of China (2021YFF0501403), the Taishan Scholars Program of Shandong Province (Zhang M and Zhang C), the Fundamental Research Funds for the Central Universities (No. 2018JC001), the Postdoctoral Science Foundation of China (2022M710084).

COMPETING INTERESTS

The authors declare no competing interests.

ETHICAL APPROVAL

All mice experiments were carried out following the general guidelines of the Association for Assessment and Accreditation of Laboratory Animal Care, as approved by the Laboratory Animal Committee of Shandong University Qilu Hospital (Jinan, Shandong Province, China). And the human investigations were in accordance with the Declaration of Helsinki, and approved by the Research Ethics Committee of Shandong University Qilu Hospital after informed consent was obtained from the patients. (Permit number: KYLL-2017(KS)-121).

ADDITIONAL INFORMATION

Supplementary information The online version contains supplementary material available at https://doi.org/10.1038/s41418-023-01115-2.

Correspondence and requests for materials should be addressed to Cheng Zhang or Meng Zhang.